Structural and Functional Changes in the αA-Crystallin R116C Mutant in Hereditary Cataracts†

Brian A. Cobb and J. Mark Petrash*

Departments of Ophthalmology and Visual Sciences and of Genetics, Washington University School of Medicine, 660 South Euclid Avenue, Box 8096, St. Louis, Missouri 63110

Received June 26, 2000; Revised Manuscript Received September 22, 2000

ABSTRACT: α-Crystallin, the major protein component of vertebrate lenses, forms a large complex comprised of two homologous subunits, αA- and αB-crystallin. It has the ability to suppress stress-induced protein aggregation in vitro, bind saturably to lens plasma membranes, and aid in light refraction through short-range ordering. Recently, a missense mutation in αA-crystallin that changes arginine 116 to a cysteine residue (R116C) was genetically linked to one form of autosomal dominant congenital cataracts. This point mutation is reported to cause structural alterations at many levels as well as a 4-fold reduction in chaperone-like activity. To extend these findings, we examined the quaternary stability of the αA R116C mutant protein and its effect on chaperone-like activity, subunit exchange, and membrane association. Homocomplexes of mutant subunits become highly polydisperse following incubation at 37 °C, reflecting the likely in vivo distribution of the complexes. Chaperone-like activity of the αA R116C mutant is approximately 4-fold lower than wild type, whether measured before or after conversion to a polydisperse population with incubation. αA R116C complexes also have a 4-fold reduced ability to exchange subunits with wild-type complexes. Finally, membrane binding capacity measurements of mutant subunits showed a 10-fold increase over wild type. Our results, in conjunction with previous reports, suggest that the changes in complex polydispersity, the reduction of subunit exchange, and increased membrane binding capacity are all potential factors in the pathogenesis of αA R116C associated congenital cataracts.

α-Crystallin, a large dynamic protein complex comprised of 30−40 copies of the A and B subunits in roughly a 3 αA to 1 αB molar ratio, can represent up to 50% of the total soluble protein in vertebrate lenses (*1*, *2*). Wild-type human αA- (WTαA)[1] and αB-crystallin (WTαB) polypeptides have molecular masses of about 20 kDa and can form homocomplexes that average 550 kDa (*3*). Each subunit shows significant sequence homology to the small heat shock protein family and has the ability to suppress stress-induced protein aggregation in vitro, reflecting a potential in vivo role in maintenance of lens transparency (*4*). Both protein subunits are known to readily exchange between soluble α-crystallin complexes in a time (>8 h) and temperature (>25 °C) dependent manner (*5*, *6*). α-Crystallin is also believed to give lenses their refractive and transparency properties through short-range ordering, which could result from repulsion between the native protein complexes (*7*−*10*). Finally, α-crystallin is known to bind subcellular elements such as intermediate filaments and plasma membranes, but the role these interactions may play in lens physiology is largely unknown (*3*, *5*, *11*, *12*).

Published results using knock-out mice suggest significant differences between αA- and αB-crystallin. Disruption of the αB gene does not result in altered lens morphology or transparency; however, disruption of the αA gene causes early onset cataract associated with accumulation of inclusion bodies containing large amounts of αB (*13*, *14*). Interestingly, the complete absence of αA in these mice does not cause congenital cataracts.

Other studies that characterized the distribution of α-crystallin in normal, aged, and cataractous lenses showed that the amount of soluble α-crystallin found in the cytoplasm of fiber cells falls steadily with increasing age and/or presence of cataract. Furthermore, these changes appear to be mirrored by an increase in the abundance of α-crystallin in the water-insoluble fraction from lens homogenates (*15*−*19*). The prevailing explanation for these observations is that the amount of soluble α-crystallin available to bind partially denatured lens proteins becomes depleted with age, and any further protein denaturation results in the formation of light scattering aggregates. It is interesting to note that the amount of crystallin protein, especially α-crystallin, bound to the fiber cell plasma membranes also increases with age and/or cataract formation (*20*, *21*). These observations suggest that there could be a common link between progressive α-crystallin

† This work was supported in part by National Institutes of Health Grants EY05856, EY02687, EY06901, and DK20579 and awards to J.M.P. and the Department of Ophthalmology and Visual Sciences from Research to Prevent Blindness, Inc.

* To whom correspondence should be addressed.

[1] Abbreviations: WTαA, wild-type αA-crystallin; WTαB, wild-type αB-crystallin; 7xHis-αA, NH_2-terminal histidine-tagged wild-type αA-crystallin; αA R116C, αA-crystallin with arginine 116 replaced with a cysteine residue; PBS, phosphate-buffered saline; CLA, chaperone-like activity; SDS−PAGE, sodium dodecyl sulfate−polyacrylamide gel electrophoresis; CD, circular dichroism; FET, fluorescence energy transfer; A_{280}, absorbance at 280 nm.

10.1021/bi001453j CCC: $19.00
Published on Web 11/23/2000

insolubilization, membrane association, and age-related loss of transparency (*21*).

Recently, a missense mutation in αA-crystallin corresponding to a change that replaces arginine 116 with a cysteine residue (αA R116C) was genetically linked to autosomal dominant congenital zonular central nuclear cataracts in humans (*22*). In that study, patients carrying the R116C mutation were shown to be heterozygous, leading to lenses that likely contained both WTαA and αA R116C. Biochemical studies indicate that the αA R116C mutation causes significant structural perturbations, including a dramatic increase in the molecular mass of the αA R116C homocomplexes (*23*, *24*). In addition, circular dichroism and tryptophan fluorescence have shown significant differences in both the secondary and tertiary structure of the mutant subunits while chaperone assays show an approximate 4-fold reduction in chaperone-like activity (CLA) as compared with WTαA (*23*, *25*). To date, it is unclear what role αA R116C may play in cataract pathogenesis; however, the current proposed mechanism suggests that reduced capacity to suppress protein aggregation may lead to the accelerated lens opacification associated with this type of congenital cataract (*25*).

In the present study, we demonstrate that homomeric complexes composed of R116C mutant subunits are of significantly higher polydispersity than homomeric complexes of WT subunits. We further show that exchange of mutant subunits into complexes containing WTαA or WTαB occurs poorly and that plasma membrane binding capacity of the mutant subunits is markedly elevated. These results, in combination with previous studies, suggest a novel mechanism for cataract formation that may include disruption of short-range ordering and increased plasma membrane association.

EXPERIMENTAL PROCEDURES

Purification and Mutagenesis of Recombinant Human αA- and αB-Crystallins. Sequences encoding human WTαA and WTαB crystallins were cloned into the pET23d expression plasmid (Novagen) and the respective recombinant proteins expressed and purified from bacterial host cultures (*Escherichia coli* strain BL21) essentially as described previously (*3*, *26*). ^{14}C-enriched proteins were prepared exactly as previously described for nonenriched proteins, except they were grown with uniformly labeled [^{14}C]glucose (Pharmacia) as the sole carbon source (625 μCi/L of culture). Mutagenesis of WTαA to R116C was performed using the QuikChange Mutagenesis kit according to the manufacturer's recommendations (Stratagene). NH_2-terminal histidine-tagged αA-crystallin (7xHis-αA) was made by subcloning of a multihistidine-encoding adapter (7xHis) in frame with the initiation codon of the wild-type cDNA in the context of the pET23d expression plasmid. Expression was performed as described for the wild-type proteins, and purification was carried out in a single step using standard nondenaturing nickel affinity procedures as described by the column resin manufacturer (Bio-Rad, Richmond, CA). Each construct was confirmed by sequencing on an ABI 310 genetic analyzer using dRhodamine dideoxy termination (Perkin-Elmer). CLA, membrane binding, and molecular mass of 7xHis-αA complexes were not significantly different from WTαA (data not shown). All proteins were estimated to be >99% homogeneous judging by the appearance of a single band following SDS−PAGE and Coomassie Blue staining. Proteins were stored at −80 °C in PBS (137 mM NaCl, 2.7 mM KCl, 4.3 mM Na_2HPO_4, 1.4 mM K_2HPO_4, pH 7.3) until use.

α-Crystallin Conjugation to AlexaFluor350 and AlexaFluor430. Purified recombinant α-crystallins were conjugated with either the AlexaFluor350 or AlexaFluor430 fluorescent tags as described by the manufacturer (Molecular Probes, Eugene, OR). Briefly, α-crystallin subunits were mixed with AlexaFluor powder in PBS supplemented with 100 mM sodium bicarbonate. Conjugation was allowed to proceed for 1 h at room temperature. The reaction was stopped with the addition of hydroxylamine. Conjugated protein was separated from nonreacted AlexaFluor reagent using a prepacked desalting column according to the manufacturer's protocol (Bio-Rad Econo-Pac 10DG column, Hercules, CA). The purified conjugates were analyzed using A_{280}/A_{346} (for AlexaFluor350) or A_{280}/A_{434} (for AlexaFluor430) readings in a Varian Cary 1E UV/vis spectrophotometer. Protein concentration and degree of conjugation (i.e., conjugation efficiency) were determined for the AlexaFluor350 conjugates using the equations:

$$[\text{protein}] = \frac{[A_{280} - (A_{346} \times 0.19)] \times \text{dilution}}{\epsilon_{\text{protein}}} \quad (1)$$

$$\text{mol of dye/mol of subunit} = \frac{A_{346} \times \text{dilution}}{19000[\text{protein}]} \quad (2)$$

where 0.19 is a correction factor for the absorbance of AlexaFluor350 at 280 nm, 19 000 is the molar extinction coefficient for AlexaFluor350, A_{280} and A_{346} are the measured absorbance values at 280 and 346 nm, respectively, and $\epsilon_{\text{protein}}$ is the molar extinction coefficient for α-crystallin. Likewise, concentration and conjugation efficiency for the AlexaFluor430 conjugates were calculated using the equations:

$$[\text{protein}] = \frac{[A_{280} - (A_{434} \times 0.28)] \times \text{dilution}}{\epsilon_{\text{protein}}} \quad (3)$$

$$\text{mol of dye/mol of subunit} = \frac{A_{434} \times \text{dilution}}{16000[\text{protein}]} \quad (4)$$

where 0.28 is a correction factor for the absorbance of AlexaFluor430 at 280 nm, 16 000 is the molar extinction coefficient for AlexaFluor430, A_{280} and A_{434} are the measured absorbance values at 280 and 434 nm, respectively, and $\epsilon_{\text{protein}}$ is the molar extinction coefficient for α-crystallin.

Lens Plasma Membrane Fractionation. Bovine lens plasma membranes were isolated and quantified as described previously (*3*). Dry weight determinations were performed in replicates of at least four.

Radioactivity Measurements. Radionuclei disintegrations of membrane-bound [^{14}C]-α-crystallin complexes were quantified using both MicroScint20 scintillation fluid and white OptiPlates in a Topcount microplate scintillation counter (Packard Instrument Co.). All other measurements were taken using ScintiVerse BD scintillation fluid (Fisher) in a Beckman LS 5000CE scintillation counter. Specific activity of radioactive proteins was determined by measuring the counts

per minute of known quantities of protein with at least eight replicates.

Extent of Subunit Exchange Measurements. The extent of subunit exchange was measured using two methods. First, ^{14}C-αA R116C was incubated for 15 h at 37 °C in PBS in either the presence or absence of WTαA. The degree of exchange was measured by resolving the crystallin complexes by FPLC using Superose 6 separation media. Column fractions were assayed for protein (A_{280}) and radioactivity (described above) to determine the elution profiles of αA R116C, WTαA, and mixed complexes produced following incubation.

A second method for measuring subunit exchange involved use of purified recombinant NH_2-terminal histidine-tagged αA-crystallin (7xHis-αA). WTαA and αA R116C (both ^{14}C-enriched) were each incubated in the presence and absence of an equimolar amount of nonradioactive 7xHis-αA for 15 h at 37 °C in PBS. Following the incubation, the protein was exchanged into nickel affinity binding buffer (5 mM imidazole, 500 mM NaCl, 20 mM Tris-HCl, pH 7.9) with a prepacked desalting column (Bio-Rad Econo-Pac 10DG column, Richmond, CA). The samples were then passed over a charged nickel affinity column. The eluate was collected, and the column was washed extensively with wash buffer (60 mM imidazole, 500 mM NaCl, and 20 mM Tris-HCl, pH 7.9) to remove any trapped complexes not directly bound to the resin. Finally, the retained α-crystallin complexes were recovered with elution buffer (1 M imidazole, 500 mM NaCl, and 20 mM Tris-HCl, pH 7.9) and then assayed for radioactivity as described above.

Fluorescence Energy Transfer Measurements. The rate of subunit exchange between WTαA and αA R116C was measured using fluorescence energy transfer (FET). AlexaFluor350-conjugated WTαA or αA R116C was used as the fluorescence donor, and AlexaFluor430-conjugated WTαA was used as the fluorescence acceptor. A total of 50 μg of the donor protein was incubated with 50 μg of either nonconjugated (no fluorescence acceptor) or conjugated (fluorescence acceptor) WTαA in PBS at 37 °C. Fluorescence intensity of the donor in the presence (F_{da}) and absence (F_d) of the acceptor was measured at various time points to determine the efficiency of transfer (E), as calculated using the equation:

$$E = 1 - (F_{da}/F_d) \quad (5)$$

E was scaled to reflect the extent of subunit exchange by first dividing each data point by the extrapolated maximum of each plot and then multiplying by the fractional extent of subunit exchange as determined by nickel affinity chromatography. The time required to reach half-completion, $T_{0.5}$, was determined through curve fit analysis and used to determine the rate of exchange. The slope between time 0 and $T_{0.5}$ was calculated for each protein combination and reported as the initial rate (V_0).

Molecular Mass Determination. Molecular masses of the wild-type and mutant homopolymers were determined using an FPLC system and a room temperature Superose 6 column as previously described (*3*).

Chaperone-like Activity Measurements. CLA measurements were collected using a heat-denaturation assay with recombinant human aldose reductase as the substrate essentially as described previously (*26*). Briefly, all assays were performed using 2 nmol of aldose reductase in PBS with a total reaction volume of 1.0 mL. The change in light scattering was monitored at 390 nm for 1 h at 52 °C using a Cary 1E UV/vis spectrometer. Heterocomplexes for CLA measurements were reconstituted by combining the subunits in the desired molar ratio in PBS and incubating at 37 °C to completion (>15 h) (*5*, *27*, *28*).

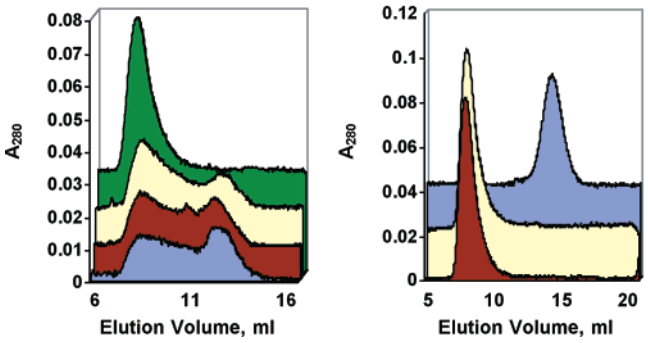

FIGURE 1: Effects of temperature and DTT on the structural organization of αA R116C homocomplexes. (A) αA R116C was incubated for various times at 37 °C and then analyzed by Superose 6 column chromatography at room temperature. (green) = 0 h, (yellow) = 24 h, (burgundy) = 48 h, and (blue) = 96 h. The data show a progressive increase in the polydispersity of the complexes, such that at >24 h complexes range in molecular mass from >4 MDa to less than 550 kDa. (B) αA R116C was run on a Superose 6 column in the presence (burgundy) or absence (yellow) of 5 mM DTT and compared to WTαA in the absence of DTT (blue). No differences were seen in the elution profile of either WTαA (with DTT not shown) or αA R116C when analyzed in the presence or absence of reducing conditions.

Membrane Binding Measurements. Membrane binding was performed essentially as previously described, except ^{14}C-enriched proteins were used to increase the assay sensitivity (*3*). Briefly, a varied amount of [^{14}C]-αA-crystallin (WT or R116C) was incubated with 500 μg of bovine cortical fiber cell plasma membranes in binding buffer (PBS supplemented with 5 mM $MgCl_2$) for 6 h at 37 °C. Following the incubation, each assay was centrifuged at 14000*g* for 30 min at 4 °C and decanted. The pellet, containing plasma membrane and bound [^{14}C]-αA-crystallin, was then analyzed for radioactivity. Using an amount of α-crystallin bound versus amount added plot, the *y*-axis intercept of the horizontal asymptote indicates the total binding capacity of each protein for these membranes.

RESULTS

Structural Stability of the αA R116C Homocomplex. To determine the size distribution of the αA R116C mutant complex at body temperature, the elution profile of αA R116C from a Superose 6 FPLC size-exclusion column was compared before and after incubations at 37 °C. This analysis revealed that the structural organization of αA R116C homocomplexes is much less defined than that of WTαA complexes (see Figure 1B for WTαA elution pattern). Freshly isolated recombinant αA R116C complexes were eluted from the column at a position corresponding to the void volume, indicating a size greater than 4 MDa. However, after incubation of the protein at 37 °C for up 96 h in PBS, substantial changes in quaternary structure were revealed (Figure 1A). After 24 h at 37 °C, the elution pattern changed

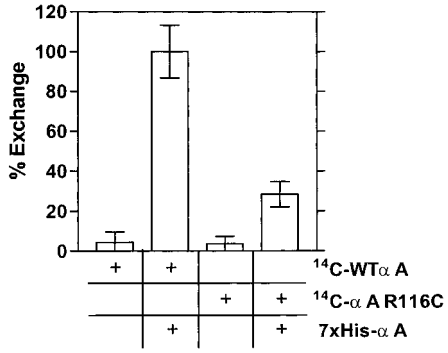

FIGURE 2: Extent of subunit exchange by nickel affinity chromatography. ^{14}C-αA R116C and ^{14}C-WTαA homocomplexes were separately incubated in the presence and absence of nonradioactive 7xHis-αA for 15 h at 37 °C. Following the incubation, samples were exchanged into nickel affinity binding buffer and then loaded onto a charged nickel affinity column. The resin was washed extensively with wash buffer and then eluted with imidazole. The counts per minute of the final eluate was measured to determine the amount of radioactive α-crystallin subunits bound to the resin as a measure of exchange into the nickel binding 7xHis-αA complexes. Data were normalized to the ^{14}C-WTαA + 7xHis-αA mixture data. The data indicate that the αA R116C subunits show an approximate 4-fold reduction in the total amount of exchange possible.

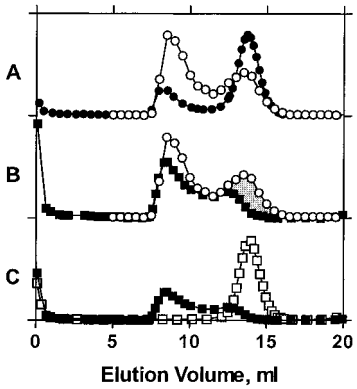

FIGURE 3: Extent of subunit exchange by Superose 6 analysis. (A) ^{14}C-αA R116C homocomplexes were incubated for 15 h at 37 °C in PBS with nonradioactive WTαA homocomplexes in a 1:1 molar ratio to allow exchange to occur. The samples were loaded onto a Superose 6 size-exclusion column for analysis. Fractions were collected and measured for absorbance at 280 nm (●) and counts per minute (○). (B) αA R116C was incubated for 15 h at 37 °C in PBS in the absence of WTαA. The elution profile using absorbance at 280 nm (■) is overlaid with the radioactivity profile (○) from panel A to demonstrate the effect of WTαA subunits on the elution of αA R116C (shaded area). (C) A_{280} profiles of WTαA (□) and αA R116C (■) after separate incubations for 15 h at 37 °C in PBS.

from a sharp peak eluting at the void volume of the column to a very polydisperse population of complexes ranging in size from greater than 4 MDa to approximately 600 kDa. These changes appear to reach equilibrium between 24 and 48 h at 37 °C. In contrast, there were no substantial changes in the elution pattern of WTαA complexes incubated for up to 96 h at 37 °C (data not shown). SDS−PAGE analysis of samples incubated for up to 4 days under these conditions demonstrated no appreciable degradation or loss of solubility (data not shown).

Since the R116C missense mutation introduced a cysteine side chain theoretically capable of participating in a disulfide bridge, we compared the elution behavior of WT and αA R116C complexes in the presence of the reducing agent dithiothreitol (DTT). WTαA eluted at a position corresponding to an average molecular mass of 550 kDa in the presence (data not shown) and absence of DTT (Figure 1B). The αA R116C homocomplexes eluted in the void volume of the column with or without DTT, indicating that the increased size of the αA R116C complexes is not due to intersubunit disulfide bridges (Figure 1B).

Extent of Subunit Exchange between αA R116C and WTαA. To determine the degree in which the mutant α-crystallin subunits mix with the wild-type αA and αB subunits that are present in individuals with this mutation, the subunit exchange between WTαA and αA R116C was assessed. First, we employed an NH_2-terminal histidine-tagged wild-type αA-crystallin (7xHis-αA). Either ^{14}C-αA R116C or ^{14}C-WTαA was incubated for 15 h at 37 °C in the presence or absence of equimolar amounts of nonradioactive 7xHis-αA. Afterward, the mixtures were passed over a charged nickel affinity column and washed as described in Experimental Procedures. The bound material was recovered with elution buffer and analyzed for radioactivity, which should be present only if radioactive subunits formed mixed complexes with the nickel binding 7xHis-αA subunits. As shown in Figure 2, neither ^{14}C-αA R116C nor ^{14}C-WTαA alone bound to the nickel affinity column. Unlike ^{14}C-WTαA, however, only a small amount of ^{14}C-αA R116C was found in the final eluate following incubation with 7xHis-αA. The total amount of bound ^{14}C-αA R116C when combined with 7xHis-αA was approximately 4-fold lower than ^{14}C-WTαA.

To further support these findings, the difference in elution behavior from a Superose 6 column was utilized. ^{14}C-αA R116C was combined in a 1:1 molar ratio with nonradioactive WTαA and incubated for greater than 15 h at 37 °C in PBS to allow the exchange to reach equilibrium. Afterward, the mixture was loaded onto a Superose 6 column and the eluate monitored by absorbance at 280 nm (A_{280}) and presence of radioactivity to determine the distribution of ^{14}C-αA R116C within the A_{280} profile (Figure 3, panel A). From these data, it appeared that some of the radioactive αA R116C subunits coeluted with the WTαA subunits. Comparison of the radioactivity profile of this mixed sample to the A_{280} profile of αA R116C incubated alone showed that while a large population of R116C homocomplexes persists (as evidenced by the material eluting near the column void volume), a small fraction of the radioactive R116C subunits exchanged into complexes that elute at a position corresponding to WTαA (see shaded area in Figure 3, panel B). This suggests that a small but detectable fraction of αA R116C subunits is capable of exchanging into complexes predominantly composed of WTαA subunits. There were no observable changes in the molecular mass of WTαA homocomplexes following overnight incubation at 37 °C (Figure 3, panel C). Similar results were obtained in exchange reactions containing ^{14}C-αA R116C and WTαB (data not shown).

Subunit Exchange Rate between αA R116C and WTαA. To extend the above subunit exchange findings, the rate of exchange was also determined. The time course of exchange for the fluorescence acceptor WTαA polypeptides (AlexaFluor430 conjugate) with the fluorescence donor WTαA or αA R116C homocomplexes (AlexaFluor350 conjugates) was measured by the change in energy transfer efficiency

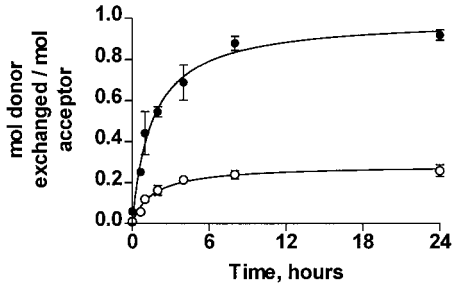

FIGURE 4: Subunit exchange rate by FET analysis. AlexaFluor350-conjugated WTαA and αA R116C (fluorescence donors) were incubated at 37 °C in PBS with either nonconjugated WTαA or AlexaFluor430-conjugated WTαA as the fluorescence acceptor. The increase in energy transfer, as calculated using eq 5, was monitored by measuring the fluorescence of the donor in the presence and absence of acceptor and then scaled as described in Experimental Procedures. WTαA subunits exchanged into WTαA (●) and αA R116C (○) homocomplexes with initial rates of $(8.7 \pm 0.2) \times 10^{-5}$ and $(2.5 \pm 0.1) \times 10^{-5}$ mol exchanged per second, respectively.

over time at 37 °C in PBS. Since the critical distance for energy transfer is between 30 and 50 Å, efficient transfer should only occur if both donor and acceptor conjugates are within a single complex. Figure 4 demonstrates that, at a 1:1 molar ratio, WTαA subunits exchanged into both WTαA and αA R116C homocomplexes, with initial rates (V_0) of $(8.7 \pm 0.2) \times 10^{-5}$ and $(2.5 \pm 0.1) \times 10^{-5}$ mol exchanged into WTαA complexes per second, respectively. This 3.5-fold reduction in rate for αA R116C is similar to the 4-fold reduction in extent of exchange. In both cases, an equilibrium was established after approximately 8 h of incubation at 37 °C.

Effect of Temperature on αA R116C CLA. Using a variety of substrate proteins at both 25 and 37 °C, previous studies have demonstrated that the R116C mutation causes a significant reduction in CLA (*23*, *25*). In light of our observations that prolonged incubation of R116C subunits at 37 °C results in substantial changes in quaternary structure, we determined whether these changes had any effect on CLA using heat-denaturation assays with human aldose reductase as the substrate. As an assay control (no preincubation), we observed an approximate 4-fold reduction in CLA for αA R116C as compared to WTαA, which agrees well with published reports (Figure 5A). This is shown by the requirement of 2.4 nmol of αA R116C to achieve 50% inhibition of aggregation instead of 0.6 nmol as seen with WTαA. After incubation for 15 h at 37 °C, however, the CLA of 0.6 nmol of WTαA (Figure 5B) and 2.4 nmol of αA R116C (Figure 5C) did not change significantly despite the structural rearrangements we observed in the αA R116C protein complex with incubation at 37 °C (see Figure 1A).

CLA of Heterocomplexes. We sought to determine if the presence of αA R116C subunits has a dominant negative effect on the CLA of the wild-type α-crystallin subunits. Complexes were formed by combining WTαA, αA R116C, and WTαB subunits in their expected in vivo ratio (1.5:1.5:1), followed by incubation at 37 °C for 15 h to allow subunit exchange to reach equilibrium (*5*, *27*, *28*). For comparison, WTαA and WTαB in the in vivo 3:1 molar ratio were incubated under the same conditions and also analyzed for CLA. We found that 0.8 nmol of the 3:1 heterocomplex was required to inhibit protein aggregation by approximately 50% (Figure 6). For the R116C-containing mixture, 1.2 nmol was needed to obtain ∼50% inhibition, which corresponds to an approximate 1.5-fold reduction in overall CLA.

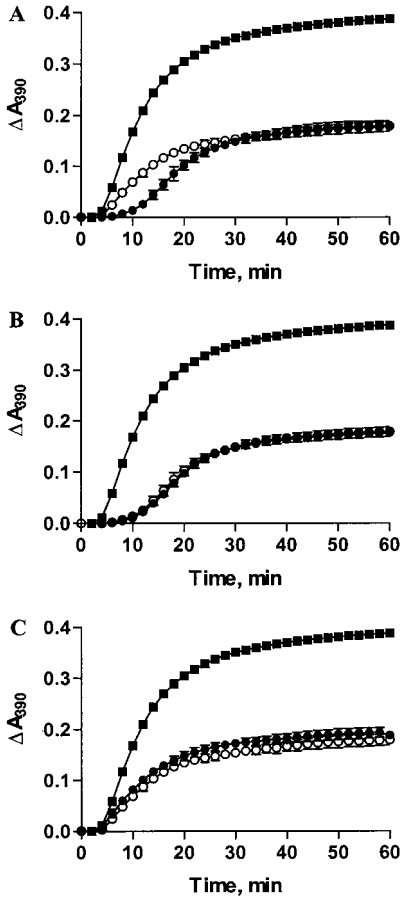

FIGURE 5: Effect of incubation on chaperone-like activity. (A) The ability to suppress ∼50% of the aggregation of 2 nmol of aldose reductase (■) at 52 °C for 0.6 nmol of WTαA (●) compared to 2.4 nmol of αA R116C (○). Light scattering was monitored at 390 nm. The data indicate that 4 times as much αA R116C is required for 50% suppression compared to the wild-type protein. (B) The CLA of 0.6 nmol of WTαA to 2 nmol of aldose reductase before (●) and after (○) a 15 h incubation at 37 °C compared to aldose reductase alone (■). The data indicate no difference between the CLA of incubated and nonincubated WTαA. (C) The CLA of 2.4 nmol of αA R116C to 2 nmol of aldose reductase before (●) and after (○) a 15 h incubation at 37 °C compared to aldose reductase alone (■). The data again indicate no difference between the CLA of incubated and nonincubated αA R116C.

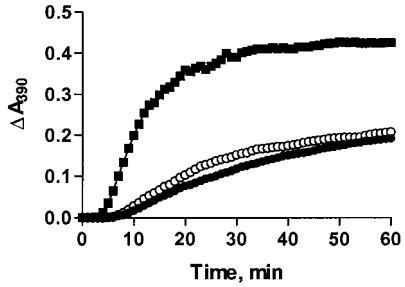

FIGURE 6: CLA of heterocomplexes. The ability to suppress the aggregation of 2 nmol of aldose reductase (■) at 52 °C in PBS for 3:1 (WTαA:WTαB) and 1.5:1.5:1 (WTαA:αA R116C:WTαB) mixed samples was compared. α-Crystallin subunits were combined and incubated at 37 °C for 15 h prior to use. The 3:1 sample assay (●) required 0.8 nmol of complex to achieve 50% inhibition of aggregation, while the 1.5:1.5:1 sample mixture (○) required 1.2 nmol of complex. These data correspond to a 1.5-fold reduction in overall CLA. Light scattering was monitored at 390 nm.

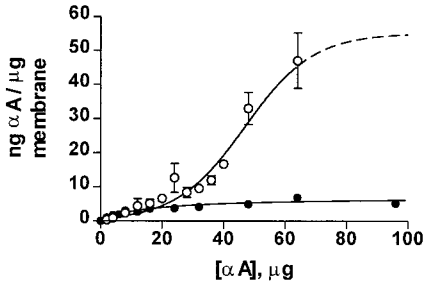

FIGURE 7: Membrane binding capacity of WTαA and αA R116C. Assays were performed using 500 μg of plasma membranes and a varied amount of either ^{14}C-WTαA or ^{14}C-αA R116C. The amount bound was calculated from the radioactivity of the membrane pellet and the specific activity for each α-crystallin complex. The binding capacity was calculated using the asymptote of each curve; values were 7.1 ± 0.7 ng of αA/μg of membrane for WTαA (●) and 55 ± 19 ng of αA/μg of membrane for αA R116C (○).

Membrane Binding Capacity of WTαA and αA R116C. We previously demonstrated that WTαA binds to lens plasma membranes in a saturable manner with an overall binding capacity of 6.6 ± 0.1 ng of WTαA/μg of membrane (*3*). To determine the effect of the R116C mutation on membrane association, binding curves were obtained using purified plasma membranes and either ^{14}C-WTαA or ^{14}C-αA R116C (Figure 7). The binding capacity for ^{14}C-WTαA was calculated to be 7.1 ± 0.7 ng of WTαA/μg of membrane, which agrees well with our previously published results (*3*). However, we observed a dramatic increase in the total amount of protein bound to the membrane in the ^{14}C-αA R116C assays. Indeed, the binding for ^{14}C-αA R116C has an estimated capacity of 55 ± 19 ng of αA R116C/μg of membrane. This corresponds to a nearly 10-fold increase over WTαA.

DISCUSSION

To gain important insight into the biochemistry of age-related cataract formation, the detailed mechanism for all types of congenital cataracts must also be well understood. In the present report, we describe important functional changes resulting from a missense mutation in αA-crystallin, R116C, which is associated with one type of congenital cataracts in humans. These perturbations suggest possible new clues about the biochemistry of these cataracts.

Some properties of the recombinant human αA R116C mutant and a "humanized" mutant of rat αA-crystallin containing the R116C substitution have been studied (*25*). We find, in concordance with previous reports, that the secondary (data not shown) and quaternary structures of homomeric complexes composed of mutant subunits are markedly different from that of WTαA and that the CLA of the αA R116C mutant is reduced approximately 4-fold. In the present study, we have extended these observations to show that, following incubation at 37 °C for 24 h or more, the quaternary arrangement of αA R116C homocomplexes becomes highly polydisperse, which likely reflects its in vivo state (Figure 1A). In addition, we show that the R116C mutation is associated with alterations in the extent and rate of subunit exchange (Figures 2−4) and markedly increased plasma membrane binding capacity (Figure 7).

A structural model based on electron spin resonance demonstrated that Arg116 in αA-crystallin (and likely Arg120 in αB-crystallin) is likely involved in a salt bridge that is buried within the complex (*29*, *30*). This suggests that removal of this residue would result in structural rearrangements due to the presence of the other charged residue buried within a low dielectric medium. This is further supported by structural characterizations of αB R120G, which demonstrate qualitatively similar alterations in the secondary, tertiary, and quaternary structures (*29*, *31*). We hypothesize that the alterations in organization of the α-crystallin complex are due in part to the destabilization of critical intersubunit interactions brought about by loss or alteration of this putative salt bridge.

A similar missense mutation in αB-crystallin (R120G) has been reported in a family with desmin-related myopathy, although there is currently no data reported that links this mutation in αB-crystallin to congenital cataracts (*32*; P. Vicart, personal communication). In addition, no studies have been reported on the subunit exchange, polydispersity, and membrane binding capacity of αB R120G. While the qualitative structural alterations and reduction in chaperone-like activity are similar for αA R116C and αB R120G, it is unclear what functional relationship exists, if any, between these mutations (*31*).

Given that the αA R116C mutation is genetically linked to a congenital cataract, we were interested in assessing the functional consequences of the structural changes seen with extended incubations at 37 °C so as to determine the validity of testing CLA without prior incubation. We found that the CLA of homocomplexes formed from αA R116C subunits was reduced approximately 4-fold relative to WTαA, regardless of the temperature or substrate conditions used to measure chaperone function, which lends support to the previous findings. Indeed, αA R116C complexes that transitioned to polydisperse complexes following incubation at 37 °C had indistinguishable CLA as compared to the previously reported activity for human αA R116C. The lack of functional changes implies that either the domain responsible for CLA is not directly affected by these rearrangements or the precise structure of that domain is not crucial for activity. Given that the CLA of α-crystallin does not involve detectable specificity to substrate proteins, it is reasonable to suggest that the hydrophilic and/or hydrophobic character of this domain is more important than a specific structural motif (*33*).

Using fluorescence energy transfer and chromatography, we have also shown that the extent and rate of subunit exchange into WTαA homocomplexes is reduced approximately 4-fold in the αA R116C protein as compared to WTαA and that even after long incubations, individual homocomplexes coexist with a relatively small number of heterocomplexes (Figures 2−4). In Figure 3, we show radioactive αA R116C subunits coeluting with the WTαA complexes only when WTαA is present. It is unlikely that this reflects CLA of WTαA toward αA R116C because denaturing proteins bound by α-crystallin shift the elution of the crystallin complex to a larger rather than smaller size. In light of these observations and with the support of the nickel affinity exchange experiment (Figure 2), the extent of radioactivity in the WT peak probably represents a rough estimate of the amount of exchange of αA R116C subunits into WTαA complexes. This suggests that complexes formed from αA R116C subunits probably exist as a population separate from wild-type α-crystallin complexes in vivo.

Individuals suffering from this autosomal dominant genetic abnormality are heterozygous for the R116C mutation, which likely leads the presence of both wild-type and mutant αA-crystallin subunits in addition to WTαB in the lens (*22*). Therefore, the reduced ability to form heterocomplexes with wild-type α-crystallin may be a key factor in understanding the dominant nature of the αA R116C mutation and its possible role in cataract formation. Due to the reduction in subunit exchange (Figures 2−4) and the lack of a dominant negative effect on the CLA of mixed populations containing αA R116C (Figure 6), it is possible that the phenotype associated with this mutation is a result of some abnormal function of the αA R116C homocomplexes that is separate from that of the heterocomplexes in affected lenses.

We have also shown for the first time that the R116C mutation results in a dramatically increased plasma membrane binding capacity (Figure 7). Given these results, it is interesting to note that the amount of α-crystallin found associated with the membrane dramatically increases with both increasing age and cataract formation (*20*, *21*). It has also been found that the amount of soluble α-crystallin decreases under the same conditions (*15*−*19*). Although it is unclear what relationship may exist between membrane binding, progressive insolubilization of α-crystallin, and cataract formation, the present results suggest that membrane association could be an important component of the opacification in age-related cataracts as well as in congenital cataracts associated with the R116C mutation.

Even more intriguing is the characterization of the αA-crystallin knock-out mice. Mice null for αA-crystallin gene expression have morphologically normal lenses at birth and develop early-onset rather than congenital cataracts (*14*). This suggests that any αA-crystallin mutation that is associated with congenital cataracts would necessarily be a gain-of-function abnormality, such as increased membrane binding, rather than a loss-of-function problem, such as reduced CLA. Due to the complete absence of WTαA in these knock-out mice, the lenses should have a dramatically reduced capacity to prevent stress-induced protein aggregation as compared to the wild-type mouse lens. Such a loss of CLA in the lens would presumably be much more severe than reducing the CLA of half the αA-crystallin subunits present by a factor of 4 (which would correspond to a theoretical 1.4-fold overall reduction) as seen with the R116C mutation. Indeed, CLA assays on mixtures of these subunits demonstrate a 1.5-fold reduction in overall CLA, indicating that αA R116C subunits do not have a dominant negative effect on (i.e., do not alter) the CLA of the wild-type α-crystallin heterocomplexes (Figure 6). Even if αA R116C subunits were the only αA-crystallin subunits present, the reduction of CLA in the lens would still be less than would be expected in the homozygous αA-crystallin knock-out mouse lens.

If reduction in CLA is not the predominant cause of congenital cataracts in individuals with the R116C mutation and if the pathogenesis involves gain-of-function abnormalities, then several possible mechanisms can be envisioned. First, it is possible that the highly polydisperse nature of the αA R116C homocomplexes could introduce major light scattering disruptions in the proposed short-range ordering of the α-crystallin complexes that is thought to be imperative for refraction and transparency (*7*−*10*). Second, this mutation might adversely affect the cytoskeletal arrangement of the intermediate filaments to which α-crystallin normally binds, resulting in improper cellular morphology and opacification (*34*−*36*). Finally, the 10-fold increase in membrane association could potentially disrupt membrane trafficking of water or other small molecules or even alter the overall order of the lipid bilayer.

Aquaporin water channels have been implicated in maintenance of lens and corneal transparency through the regulation of water movement (*37*−*40*). In fact, another type of congenital cataract has been linked to a mutation in aquaporin 0 (MiP26), the major protein component of fiber cell plasma membranes (*37*). In addition, the extremely high concentration (∼60 mol % of total lipid) of cholesterol in the nuclear plasma membranes suggests that the stability of the bilayer might also be important for lens transparency (*41*, *42*). Reduction in cholesterol synthesis increases the risk for cataract formation, and it has also been shown that high concentrations of cholesterol reduce the binding capacity of α-crystallin for the membrane (*43*, *44*). Thus, if cholesterol is reduced, then more α-crystallin should be able to associate with the membrane. The coincidence of increased membrane association of crystallin proteins and cataract formation lends support to a general proposal in which abnormal membrane association of α-crystallin could be a common feature seen in many forms of cataract, including the αA R116C associated congenital cataract.

Our studies have shown that the αA R116C homocomplex is highly polydisperse at body temperature, that the membrane binding is dramatically increased, and that the subunit exchange is reduced 4-fold. When interpreted in the context of previous studies on wild-type and R116C αA-crystallin and cataract pathogenesis, these results suggest a role for membrane association and complex polydispersity in the pathogenesis of congenital cataracts associated with the R116C missense mutation of αA-crystallin.

ACKNOWLEDGMENT

We thank Dr. Steven Bassnett, Dr. Linda Pike, and Lori Kreisman for critically reviewing the manuscript. We also thank Kent Morris and Anthony Webb for assistance in making the 7xHis-αA and αA R116C constructs, respectively.

REFERENCES

1. Bloemendal, H. (1981) in *Molecular and Cellular Biology of the Eye Lens*, pp 221−278, John Wiley & Sons, New York.
2. Gopalakrishnan, S., and Takemoto, L. (1992) *Invest. Ophthalmol. Vis. Sci. 33*, 2936−2941.
3. Cobb, B. A., and Petrash, J. M. (2000) *J. Biol. Chem. 275*, 6664−6672.
4. Horwitz, J. (1992) *Proc. Natl. Acad. Sci. U.S.A. 89*, 10449−10453.
5. Bova, M. P., Ding, L. L., Horwitz, J., and Fung, B. K. (1997) *J. Biol. Chem. 272*, 29511−29517.
6. Sun, T. X., Akhtar, N. J., and Liang, J. N. (1998) *FEBS Lett. 430*, 401−404.
7. Xia, J. Z., Aerts, T., Donceel, K., and Clauwaert, J. (1994) *Biophys. J. 66*, 861−872.
8. Xia, J. Z., Wang, Q., Tatarkova, S., Aerts, T., and Clauwaert, J. (1996) *Biophys. J. 71*, 2815−2822.
9. Veretout, F., Delaye, M., and Tardieu, A. (1989) *J. Mol. Biol. 205*, 713−728.
10. Delaye, M., and Tardieu, A. (1983) *Nature 302*, 415−417.

11. Liang, P., and Macrae, T. H. (1997) *J. Cell Sci. 110*, 1431−1440.
12. Fleschner, C. R., and Cenedella, R. J. (1992) *Curr. Eye Res. 11*, 739−752.
13. Brady, J. P., and Wawrousek, E. F. (1998) *Invest. Ophthalmol. Vis. Sci. 39*(4), S523 (Abstract 4200).
14. Brady, J. P., Garland, D., Duglas-Tabor, Y., Robison, W. G. J., Groome, A., and Wawrousek, E. F. (1997) *Proc. Natl. Acad. Sci. U.S.A. 94*, 884−889.
15. Babizhayev, M. A., Bours, J., and Utikal, K. J. (1996) *Ophthal. Res. 28*, 365−374.
16. Bessems, G. J., De, M. B., Bours, J., and Hoenders, H. J. (1986) *Exp. Eye Res. 43*, 1019−1030.
17. Bessems, G. J., Hoenders, H. J., and Wollensak, J. (1983) *Exp. Eye Res. 37*, 627−637.
18. Bindels, J. G., Bours, J., and Hoenders, H. J. (1983) *Mech. Aging Dev. 21*, 1−13.
19. Bours, J., Fodisch, H. J., and Hockwin, O. (1987) *Ophthal. Res. 19*, 235−239.
20. Boyle, D. L., and Takemoto, L. (1996) *Curr. Eye Res. 15*, 577−582.
21. Cenedella, R. J., and Fleschner, C. R. (1992) *Curr. Eye Res. 11*, 801−815.
22. Litt, M., Kramer, P., LaMorticella, D. M., Murphey, W., Lovrien, E. W., and Weleber, R. G. (1998) *Hum. Mol. Genet. 7*, 471−474.
23. Kumar, L. V., Ramakrishna, T., and Rao, C. M. (1999) *J. Biol. Chem. 274*, 24137−24141.
24. Cobb, B. A., and Petrash, J. M. (2000) *Exp. Eye Res. 71*(S1), S46 (Abstract 149).
25. Shroff, N. P., Cherian-Shaw, M., Bera, S., and Abraham, E. C. (2000) *Biochemistry 39*, 1420−1426.
26. Andley, U. P., Mathur, S., Griest, T. A., and Petrash, J. M. (1996) *J. Biol. Chem. 271*, 31973−31980.
27. Sun, T. X., and Liang, J. N. (1998) *J. Biol. Chem. 273*, 286−290.
28. van den Oetelaar, P. J., van Someren, P. F., Thomson, J. A., Siezen, R. J., and Hoenders, H. J. (1990) *Biochemistry 29*, 3488−3493.
29. Perng, M. D., Muchowski, P. J., van den IJssel, P., Wu, G. J., Hutcheson, A. M., Clark, J. I., and Quinlan, R. A. (1999) *J. Biol. Chem. 274*, 33235−33243.
30. Berengian, A. R., Bova, M. P., and Mchaourab, H. S. (1997) *Biochemistry 36*, 9951−9957.
31. Bova, M. P., Yaron, O., Huang, Q., Ding, L., Haley, D. A., Stewart, P. L., and Horwitz, J. (1999) *Proc. Natl. Acad. Sci. U.S.A. 96*, 6137−6142.
32. Vicart, P., Caron, A., Guicheney, P., Li, Z., Prevost, M. C., Faure, A., Chateau, D., Chapon, F., Tome, F., Dupret, J. M., Paulin, D., and Fardeau, M. (1998) *Nat. Genet. 20*, 92−95.
33. Velasco, P. T., Lukas, T. J., Murthy, S. N., Duglas-Tabor, Y., Garland, D. L., and Lorand, L. (1997) *Exp. Eye Res. 65*, 497−505.
34. FitzGerald, P. G., and Graham, D. (1991) *Curr. Eye Res. 10*, 417−436.
35. Carter, J. M., Hutcheson, A. M., and Quinlan, R. A. (1995) *Exp. Eye Res. 60*, 181−192.
36. Perng, M. D., Cairns, L., van den IJssel, P., Prescott, A., Hutcheson, A. M., and Quinlan, R. A. (1999) *J. Cell Sci. 112*, 2099−2112.
37. Shiels, A., and Bassnett, S. (1996) *Nat. Genet. 12*, 212−215.
38. Mitton, K. P., Kamiya, T., Tumminia, S. J., and Russell, P. (1996) *J. Biol. Chem. 271*, 31803−31806.
39. Li, J., Kuang, K., Nielsen, S., and Fischbarg, J. (1999) *Invest. Ophthalmol. Vis. Sci. 40*, 1288−1292.
40. Fischbarg, J., Diecke, F. P., Kuang, K., Yu, B., Kang, F., Iserovich, P., Li, Y., Rosskothen, H., and Koniarek, J. P. (1999) *Am. J. Physiol. 276*, C548−C557.
41. Borchman, D., Cenedella, R. J., and Lamba, O. P. (1996) *Exp. Eye Res. 62*, 191−197.
42. Duindam, J. J., Vrensen, G. F., Otto, C., and Greve, J. (1998) *Invest. Ophthalmol. Vis. Sci. 39*, 94−103.
43. Tang, D., Borchman, D., Yappert, M. C., and Cenedella, R. J. (1998) *Exp. Eye Res. 66*, 559−567.
44. Cenedella, R. J. (1996) *Surv. Ophthalmol. 40*, 320−337.

BI001453J